JOURNAL OF VIROLOGY, Nov. 2008, p. 11331–11343 Vol. 82, No. 22
0022-538X/08/$08.00+0 doi:10.1128/JVI.00577-08

Expression of Nonstructural Rotavirus Protein NSP4 Mimics Ca^{2+} Homeostasis Changes Induced by Rotavirus Infection in Cultured Cells[▽]

Yuleima Díaz,[1] Maria Elena Chemello,[1] Franshelle Peña,[1] Olga Carolina Aristimuño,[1] Jose Luis Zambrano,[2] Hector Rojas,[3] Fulvia Bartoli,[4] Leiria Salazar,[4] Serge Chwetzoff,[5] Catherine Sapin,[5] Germain Trugnan,[5] Fabian Michelangeli,[1]* and Marie Christine Ruiz[1]*

Laboratorio de Fisiología Gastrointestinal,[1] Laboratorio de Biología de Virus,[2] Laboratorio de Fisiología Celular,[3] and Laboratorio de Biología Molecular,[4] Instituto Venezolano de Investigaciones Científicas (IVIC), Apartado 21827, Caracas 1020A, Venezuela, and INSERM U 538, CHU Saint Antoine, Université Pierre et Marie Curie, 75012 Paris, France[5]

Received 14 March 2008/Accepted 28 July 2008

Rotavirus infection modifies Ca^{2+} homeostasis, provoking an increase in Ca^{2+} permeation, the cytoplasmic Ca^{2+} concentration ($[Ca^{2+}]_{cyto}$), and total Ca^{2+} pools and a decrease in Ca^{2+} response to agonists. A glycosylated viral protein(s), NSP4 and/or VP7, may be responsible for these effects. HT29 or Cos-7 cells were infected by the SA11 clone 28 strain, in which VP7 is not glycosylated, or transiently transfected with plasmids coding for NSP4-enhanced green fluorescent protein (EGFP) or NSP4. The permeability of the plasma membrane to Ca^{2+} and the amount of Ca^{2+} sequestered in the endoplasmic reticulum released by carbachol or ATP were measured in fura-2-loaded cells at the single-cell level under a fluorescence microscope or in cell suspensions in a fluorimeter. Total cell Ca^{2+} pools were evaluated as $^{45}Ca^{2+}$ uptake. Infection with SA11 clone 28 induced an increase in Ca^{2+} permeability and $^{45}Ca^{2+}$ uptake similar to that found with the normally glycosylated SA11 strain. These effects were inhibited by tunicamycin, indicating that inhibition of glycosylation of a viral protein other than VP7 affects the changes of Ca^{2+} homeostasis induced by infection. Expression of NSP4-EGFP or NSP4 in transfected cells induced the same changes observed with rotavirus infection, whereas the expression of EGFP or EGFP-VP4 showed the behavior of uninfected and untransfected cells. Increased $^{45}Ca^{2+}$ uptake was also observed in cells expressing NSP4-EGFP or NSP4, as evidenced in rotavirus infection. These results indicate that glycosylated NSP4 is primarily responsible for altering the Ca^{2+} homeostasis of infected cells through an initial increase of cell membrane permeability to Ca^{2+}.

Rotavirus is the major etiological agent of viral gastroenteritis in children and young animals (22). Rotaviruses infect enterocytes of the middle and upper epithelium of the small intestine in vivo, inducing cell death and perturbation of ionic homeostasis. The generation of rotavirus diarrhea is a multifactorial process involving Ca^{2+}-dependent secretory processes of mediators, water, and electrolytes, as well as the induction of cell death in the different cell types that compose the intestinal epithelium (27, 36). The discovery of the functioning of the nonstructural viral protein NSP4 as a viral enterotoxin and of the possible participation of the enteric nervous system in the pathogenesis of diarrhea represents a significant advance in its understanding (3, 24, 30, 31). The enterotoxin hypothesis is strengthened by the finding that a peptide (NSP4 amino acids [aa] 112 to 175) containing the enterotoxic domain of the protein, or the full-length molecule, is secreted into the bathing medium during infection (9, 47). NSP4 or the secreted peptide would bind to plasma membrane receptors in distant cells, activating the phospholipase C-IP3 signaling cascade, thereby releasing Ca^{2+} from the endoplasmic reticulum (ER) (14, 31, 43).

Rotavirus entry, activation of transcription, morphogenesis, cell lysis, particle release, and the distant action of viral proteins are Ca^{2+}-dependent processes. In the extracellular medium, Ca^{2+} stabilizes the structure of the viral capsid (35, 40). The entry of rotavirus into the cell is accompanied by the loss of the outer protein layer (VP4 and VP7) and the activation of viral transcription, probably due to the low Ca^{2+} concentration in the cytoplasm (~100 nM) (11, 13, 23). During replication, non-membrane-bound cytoplasmic inclusions (viroplasms) are formed. Synthesized viral proteins and the double-stranded RNA genome are assembled to form the new double-layered particles (DLPs) in these structures (1). DLPs interact with the cytoplasmic domain of NSP4, an integral ER membrane protein, which acts as an intracellular receptor in the budding of DLPs into the ER lumen. At this point, the outer capsid proteins VP7 and VP4 are assembled onto the DLPs, resulting in the formation of triple-layered particles within the ER lumen, the main Ca^{2+} store of the cell (2, 4, 15, 25). Depletion of calcium stored in the ER by different experimental maneuvers causes an abnormal accumulation of membrane-enveloped intermediates, which are not infectious (26, 33, 38, 39).

Mature virus is thought to be accumulated in the ER and then released by cell lysis through a Ca^{2+}-dependent mechanism in MA104 cells (28). However, in differentiated and po-

* Corresponding author. Mailing address for M. C. Ruiz: Laboratorio de Fisiología Gastrointestinal, IVIC, Caracas 1020A, Venezuela. Phone: 58 212 5041164. Fax: 58 212 5041093. E-mail: mclr@ivic.ve. Mailing address for F. Michelangeli: Laboratorio de Fisiología Gastrointestinal, IVIC, Caracas 1020A, Venezuela. Phone: 58 212 5041396. Fax: 58 212 5041093. E-mail: fabian@ivic.ve.

▽ Published ahead of print on 10 September 2008.

larized Caco2 cells, rotavirus particles seem to be released at the apical pole of the cell before cell death (21).

In addition to the dependence of virus maturation on the Ca^{2+} concentrations of different cellular compartments, infection by itself induces changes in the calcium homeostasis of the cell that may be advantageous to virus replication (26, 28). Among these perturbations, we have measured a progressive increase in plasma membrane Ca^{2+} permeability, which leads to an elevation of the cytoplasmic Ca^{2+} concentration ($[Ca^{2+}]_{cyto}$) and enhancement of sequestered Ca^{2+} pools in the ER, measured as $^{45}Ca^{2+}$ uptake sensitive to thapsigargin (26, 28). Infection also leads to a progressive depletion of agonist-mobilizable ER pools compatible with an increase in the Ca^{2+} buffering capacity within the ER (37).

The viral product responsible for the changes in Ca^{2+} homeostasis is not known. The fact that tunicamycin inhibits the increase of plasma membrane Ca^{2+} permeability induced by infection suggests that a glycosylated viral protein(s), NSP4 and/or VP7, is involved in this effect (37). NSP4 appears to be a likely candidate given its many effects on Ca^{2+} homeostasis. The expression of recombinant NSP4 in insect cells (Sf9) induced a change in the Ca^{2+} concentration, which has been interpreted as a consequence of an increase in the Ca^{2+} permeability of the ER membrane, but not of the plasma membrane (43, 44). Furthermore, the inducible intracellular expression of the NSP4-enhanced green fluorescent protein (EGFP) fusion protein in mammalian HEK 293 cells elevates basal intracellular calcium levels more than twofold by a phospholipase C-independent mechanism (6).

The studies performed so far do not provide an explanation of how the $[Ca^{2+}]_{cyto}$ increases as a result of rotavirus infection or the expression of NSP4. Furthermore, the participation of the other glycosylated viral protein, VP7, has not yet been ruled out. In the present paper, we report the effects on Ca^{2+} homeostasis of (i) infection with the rotavirus SA11 clone 28, which has an unglycosylated form of VP7, and (ii) expression of NSP4-EGFP and NSP4 in transfected Cos-7 cells.

MATERIALS AND METHODS

Cell cultures and virus infection. Cos-7 cells (derived from African green monkey kidney), MA104 cells (derived from rhesus monkey kidney), and the colon carcinoma cells HT29 (from the ATCC) were used. Cos-7 and MA104 cells were grown in minimal essential medium (MEM) (Gibco catalog no. 61100) and HT29 cells in Dulbecco's modified Eagle medium (containing 4,500 mg/liter glucose; Gibco catalog no. 12100) and were maintained as previously described (26).

The bovine rotavirus strain RF (kindly supplied by J. Cohen, CNRS, Gif sur Yvette, France) and the simian wild-type (WT) SA11 (clone 3) and the variant SA11 (clone 28) (kindly supplied by M. K. Estes, Baylor, TX) were used.

Rotaviruses were replicated in MA104 cells as described previously (37). The infectivities of the preparations were measured by titration in microplates in MA104 cells using a monoclonal antibody (4B2D2) directed against a common group A antigen of VP6 (kindly supplied by F. Liprandi) for indirect immunofluorescence staining after methanol fixation and were expressed as fluorescent focus units (12).

Plasmids and transfection experiments. The bovine RF strain NSP4 full-length cDNA was obtained by PCR using pBS-RF10 as a template (a gift of A. Charpilienne, CNRS, Gif sur Yvette, France). One primer corresponded to the 5′ end of the NSP4 sequence with a BglII site (underlined): 5′-AGATCTATG GAAAAGCTTACCGACCTCAAC-3′. The second primer corresponded to the 3′ end of the NSP4 sequence with an EcoRI site (underlined): 5′-CAGAATTC GCATCGCTGCAGTCACTTCTTTTGG-3′. The amplicon was ligated into a pEGFP-N1 vector (Ozyme, Montigny le Bretonneux, France) previously digested with BglII and EcoRI enzymes. Thus, EGFP was linked to NSP4 at the C-terminal end of the viral protein through a linker of 17 aa coded by the following nucleotide sequence: 5′-CGAATTCTGCAGTCGACGGTACCGCG GGCCCGGGATCCACCGGTCGCCACC-3′.

In order to determine whether green fluorescent protein (GFP) affected Ca^{2+} changes per se in transfected cells, a plasmid was prepared using the same pEGFP-N1 vector (Clontech), in which GFP was eliminated by EcoRI and XbaI digestions and replaced by NSP4. Primers for NSP4 were designed, including the EcoRI and XbaI sites, respectively. The forward primer corresponded to the 5′ end of the NSP4 sequence with an EcoRI site (underlined), 5′-CGAATTCAT GGAAAAGCTTACCGACCTCAA-3′, and the reverse primer corresponded to the 3′ end of the NSP4 sequence with an XbaI site (underlined), 5′-GCTC TAGATCACATCGCTGCAGTCACTTCTTTTG-3′. As the XbaI site of pEGFP-N1 was methylated, the vector was first transformed into a bacterial strain, GM2163 (New England Biolabs), and fresh DNA was prepared. Double digestions with EcoRI and XbaI of the NSP4 PCR product and the pEGFP-N1 vector were carried out, not simultaneously, but in sequence to facilitate the cleavage of DNA. The amplicon was ligated into the vector lacking GFP, and transformation was performed in XL1-Blue cells.

Plasmid transfections in Cos-7 cells were performed using Lipofectamine 2000 (Invitrogen) according to the manufacturer's instructions. Transfections of Cos-7 cells were also performed with the commercial pEGFP-N1 vector (Clontech) or the pEGFP-C1-VP4 plasmid (18).

Analysis of protein expression by immunoprecipitation and Western blotting. Cells were disrupted in a lysis buffer containing 10 mM Tris-HCl, pH 7.8, 100 mM NaCl, 0.1% NP-40, and antiprotease cocktail (10%; Sigma) and passed six times through a 23-gauge needle. To immunoprecipitate NSP4 and NSP4-EGFP, 1 μl of rat polyclonal serum raised against purified C90, a polypeptide that contains the carboxy-terminal 90 amino acid residues of purified NSP4 (kindly provided by J. A. Taylor, Auckland, New Zealand), was added to 100 μl of cell lysate supernatant and incubated overnight at 4°C. The immune complexes were captured with protein G-Sepharose beads and washed in lysis buffer. Then, they were suspended in Laemmli sample buffer with 50 mM dithiothreitol, boiled for 5 min, and then subjected to 10% sodium dodecyl sulfate-polyacrylamide gel electrophoresis (SDS-PAGE). The proteins were transferred onto a nitrocellulose membrane, and the membrane was blocked with 5% nonfat milk in phosphate-buffered saline (PBS) containing 0.05% Tween 20 overnight. NSP4 and NSP4-EGFP were identified using different primary antibodies: mouse monoclonal antibody B4-2 (kindly provided by H. Greenberg, Stanford, CA), rabbit polyclonal serum against β-galactosidase NSP4 fusion protein (kindly provided by J. A. Taylor, Auckland, New Zealand), and an anti-GFP antibody (Sigma). The secondary antibodies used were goat anti-rabbit or goat anti-mouse immunoglobulin G conjugated with horseradish peroxidase (Sigma) that was detected by chemiluminescence using the ECL kit according to the manufacturer's instructions (Pierce, Thermo Scientific).

Endo-H digestion. Samples of the cell lysate (9 μl) were incubated in denaturing buffer for 10 min at 100°C. Then, 1.5 μl of buffer containing 50 mM sodium citrate (pH 5.5) and endo-*N*-acetylglucosaminidase H (endo-H) (1,000 U; Biolab) was added, and the reaction mixture was incubated at 37°C for 1 h. Proteins were analyzed by Western blotting as described above.

Determination of intracellular Ca^{2+} concentrations in cell suspensions. HT29 and Cos-7 cells were seeded on 75-cm^2 Falcon flasks at a density of 300,000 cells/flask in MEM supplemented with 10% fetal calf serum and were used at confluence 5 to 7 days later. The monolayers were infected by SA11 (WT or clone 28) rotavirus at a multiplicity of infection of 20 fluorescent focus units/cell. At the end of the infection period, the cells were detached from the flask by trypsin treatment, washed by centrifugation, and resuspended at an approximate concentration of 8×10^6 cells/ml in a medium containing (in mM) NaCl, 130; KCl, 5; $CaCl_2$, 1; $MgCl_2$, 1; HEPES, 20 (pH 7.2); and 0.1% (wt/vol) albumin. The cell suspensions were incubated with 5 μM fura-2–AM with Pluronic (0.01%) for 30 min, washed twice by centrifugation, resuspended in buffer, and maintained at room temperature. For measurements, aliquots of the cell suspension were newly washed and resuspended in 1.2 ml of the same medium without albumin. Fluorescence was measured at 37°C in a spectrofluorimeter (Photon Technology International) equipped with a stirrer and temperature control. The excitation wavelengths were 340 and 380 nm, which were alternately changed by computer control, allowing acquisition of one pair of data per second. Emission was fixed at 510 nm. The ratio of the fluorescent signals measured at 340 and 380 nm was determined by computer. The intracellular free-Ca^{2+} concentration, $[Ca^{2+}]_{cyto}$, was calculated according to the equation described by Grynkiewicz et al. (20), using an apparent K_d (dissociation constant) for fura-2/Ca of 224 nM. The maximal fluorescence ratio was determined by the addition of digitonin (80 μg/ml) to permeabilize the cells, and the minimal fluorescence ratio was deter-

mined by the subsequent addition of 20 mM EGTA in Tris (0.1 M), pH 7.4, buffer.

Measurements of $[Ca^{2+}]_{cyto}$ in single cells. Cos-7 cells grown on glass coverslips were infected or transfected as described above. RF rotavirus-infected cells were used at 8 h postinfection and transfected cells at 24 to 30 h posttransfection. Cell monolayers were incubated for 30 min at room temperature with 5 μM fura-2–AM. Coverslips were mounted in a flowthrough perfusion microscope chamber (Warner Instruments). The cells were superfused with Ringer medium containing (in mM) NaCl, 145; KCl, 5; $MgSO_4$, 1; $CaCl_2$, 1.8; glucose, 11; HEPES, 20 (pH 7.45); and mosmol/liter, 310. Solutions containing different Ca^{2+} concentrations and/or agonists were rapidly changed using a computerized perfusion system (DAD-12; ALA Scientific Instruments Inc., New York, NY).

Fluorescence imaging and photometry of fura-2-loaded cells were performed using an inverted fluorescence microscope (Nikon TE-300) equipped with a cooled charge-coupled device camera (Newcastle Photometric Systems), shutters, and a filter wheel for excitation wavelength changes. Fluorescence was measured from up to 16 preselected regions at 16-bit resolution. In the case of transfected cells, these were selected in a fluorescence image obtained with a 40× oil immersion (1.3-numerical-aperture) objective at excitation/emission wavelengths of 500/535 nm to visualize the NSP4-EGFP fusion protein. Measurements were performed in cells emitting a diffuse NSP4-EGFP fluorescence with an intermediate intensity. Infected cells were randomly selected.

For Ca^{2+} measurements, fura-2-loaded cells were alternatively illuminated at excitation wavelengths of 350 and 380 nm, and fluorescence was recorded at 535 nm. All measurements were made at room temperature. Fluorescence data are expressed as the following ratio: (F350 − F background 350)/(F380 − F background 380), where F350 and F380 are the values for cell fluorescence, measured with excitations of 350 and 380 nm, respectively. Control experiments performed with NSP4-EGFP-expressing cells not loaded with fura-2 showed that, at the wavelengths selected for fura-2 fluorescence measurements (excitation, 350 nm/380 nm; emission, 535 nm), neither a fluorescence signal nor changes in intensity were detected when 5 mM Ca^{2+} was added to the medium. This indicates that, in our experimental setup, there was no contribution of EGFP fluorescence to the fura-2 signal.

$^{45}Ca^{2+}$ uptake. The cell uptake of $^{45}Ca^{2+}$ was measured in rotavirus-infected or -transfected Cos-7 cells as previously described (28). Briefly, cell monolayers were grown to confluence in 24-well Linbro plates for 3 to 4 days and infected (multiplicity of infection, 20) or transfected as described above. At the end of the infection (8 h) or transfection (24 h), the maintenance medium was removed and replaced by 200 μl of MEM containing $^{45}Ca^{2+}$ (1 μCi per well). Uptake was stopped after 10 min by washing the cells four times by immersion in ice-cold PBS. After air drying, cells were dissolved in 250 μl of 0.1% SDS. Radioactivity was determined in aliquots by liquid scintillation counting. As the number of cells per well was found to be constant, uptake values for single experiments were normalized and expressed as the ratio to counts obtained under mock-infected or transfected conditions, respectively.

Immunofluorescence and confocal microscopy. Cos-7 cells were grown to 90% confluence on glass coverslips and infected with the RF strain of rotavirus or transfected with different plasmids for the transient expression of EGFP, NSP4, or NSP4-EGFP. The cells were washed in PBS and fixed at 7 h postinfection or at 24 h posttransfection with 2% paraformaldehyde in PBS for 20 min at room temperature, with subsequent permeabilization with 0.3% Triton X-100 in PBS for 10 min. The cells were incubated with primary antibody against NSP4 (B4-2; kindly provided by H. Greenberg, Stanford, CA) diluted in PBS with 50 mM NH_4Cl (1 h at 37°C) and then washed and incubated with Cy3- or fluorescein isothiocyanate-labeled secondary anti-mouse immunoglobulin (Sigma) for 2 h at 37°C.

The dual-labeled cells were viewed on either a Nikon or a Leica confocal system. The Nikon spectral laser scanning confocal system (Nikon C1) was mounted in an Eclipse TE300 Nikon inverted microscope using a Nikon 60/1.40 PlanApo oil immersion objective and coupled to a C1-LU2 laser unit with neon (543-nm) and argon (488-nm) air-cooled lasers. This laser unit was controlled by a D-eclipse C1 interface. The Leica TCS Spectral (SP2) instrument was equipped with an inverted microscope with 63× and 100× oil immersion objectives, both with a numerical aperture of 1.4. A krypton-argon mixed-gas laser and two helium-neon mixed-gas lasers were used to generate the bands at 488 nm, 543 nm, and 633 nm, respectively.

RESULTS

Role of VP7 in changes of Ca^{2+} homeostasis in infected cells. We have shown that tunicamycin and cycloheximide inhibit the increase of plasma membrane Ca^{2+} permeability induced by infection. However, this increase was not affected by actinomycin D, ruling out the participation of a newly synthesized cellular protein and suggesting that a glycosylated viral protein(s), NSP4 and/or VP7, is involved in this effect (26, 28, 37). We have proposed that the responsible viral glycoprotein(s) travels to the plasma membrane to form a Ca^{2+} channel and hence elevate Ca^{2+} permeability (37). Therefore, we first evaluated the participation of glycosylated VP7 in this effect. The strategy used was to compare changes in Ca^{2+} homeostasis in cells infected by the WT rotavirus (SA11 WT) or by a variant of SA11 defective in glycosylation of VP7 (SA11 clone 28; kindly provided by M. K. Estes). These experiments were performed in HT29 and Cos-7 cells, where the expressed forms of both clones were previously analyzed by SDS-PAGE, confirming the same pattern described by Estes et al. (reference 16 and data not shown).

We studied the relationship between infection, Ca^{2+} permeability, and agonist-releasable Ca^{2+} pools in fura-2-loaded cells in a fluorimeter cuvette. Individual traces of $[Ca^{2+}]_{cyto}$ from a representative experiment performed with HT29 cells are presented in Fig. 1, and the analyses of two experimental series performed with HT29 and Cos-7 cells are shown in Fig. 2. Plasma membrane permeability was evaluated by measuring $[Ca^{2+}]_{cyto}$ and calculating the initial rate of change ($d[Ca^{2+}]/dt$) attained after the addition of 5 mM Ca^{2+} to the medium.

An increase in basal $[Ca^{2+}]_{cyto}$ was observed in HT29 cells infected by WT or SA11 clone 28 rotavirus (Fig. 1). In a series of four experiments, this increase was significant (mock infected, 181 ± 12 nM; SA11 WT, 239 ± 16 nM; and SA11 clone 28, 280 ± 20 nM). Similar results were obtained in Cos-7 cells; however, they did not reach a level of significance at this time postinfection. The addition of Ca^{2+} (5 mM) to the extracellular medium induced an increase of $[Ca^{2+}]_{cyto}$ in HT29 cells infected by either of the two clones, whereas almost no change was observed in uninfected cells (Fig. 1A). The statistical analysis of this event shows that the initial rate and amplitude of the increase were significant for HT29 or Cos-7 cells infected by the two SA11 virus clones (Fig. 2A to D). The comparison of the effects obtained with the two clones revealed a significantly higher increase for cells infected with the SA11 clone 28 virus in HT29 cells (Fig. 1A and 2A). However, this difference was not observed in Cos-7 cells (Fig. 2B).

An indirect way to estimate the state of filling of ER Ca^{2+} deposits is to evaluate the ability of the agonist to mobilize sequestered Ca^{2+} pools through the activation of the phospholipase C-IP3 signaling chain. When carbachol was added to HT29 cells, it caused a fast rise in $[Ca^{2+}]_{cyto}$ in all cases. The amplitude of the Ca^{2+} response in rotavirus-infected cells was the same independent of the SA11 clone used but significantly smaller than that observed in uninfected cells (Fig. 1B and 2E). Similar results were obtained with infected Cos-7 cells when ATP was used as the agonist to activate purinergic receptors and to mobilize Ca^{2+} from the ER (Fig. 2F).

It is known that the depletion of ER Ca^{2+} by an agonist activates Ca^{2+} entry through store-operated channels or the so-called capacitative pathway. Since rotavirus infection progressively depletes the agonist-releasable pool, it was necessary to evaluate the contribution of the capacitative pathway to overall Ca^{2+} permeability. Addition of 5 mM Ca^{2+} to the

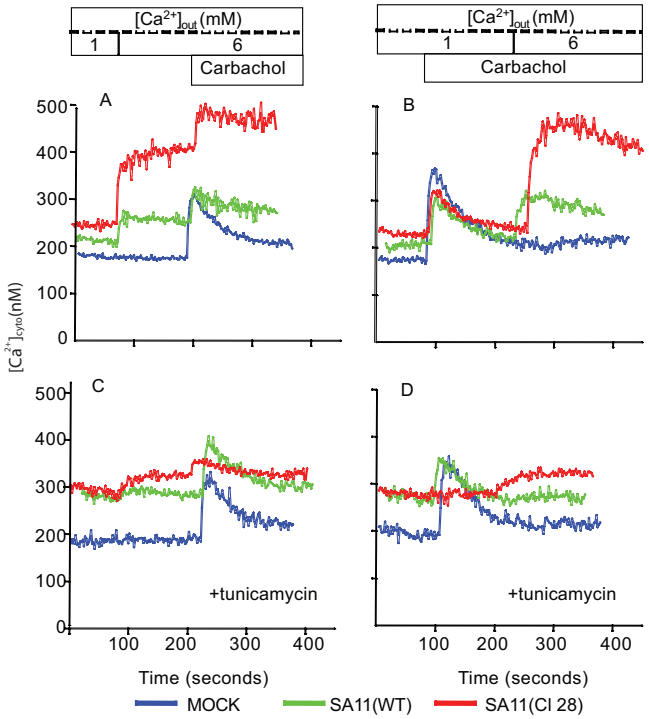

FIG. 1. Effects of rotavirus infection with the WT and variant clone 28 (Cl 28) SA11 strains on $[Ca^{2+}]_{cyto}$, plasma membrane permeability to Ca^{2+}, and agonist-releasable Ca^{2+} pools in HT29 cells. Confluent monolayers of HT29 cells grown in 75-cm^2 Falcon flasks were infected with the WT or the variant clone 28 of SA11 rotavirus. A mock-infected flask was kept as a control. At 1 h postinfection the inoculum was removed and replaced by fresh medium (A and B) or medium containing 5 μg/ml tunicamycin (C and D). At 6 h postinfection, the monolayers were trypsinized, and the cell suspensions were loaded with fura-2 for measurement of the $[Ca^{2+}]_{cyto}$ in a fluorimeter cuvette. Under all conditions (with [+] or without tunicamycin treatment), membrane permeability to Ca^{2+} was evaluated by the change in $[Ca^{2+}]_{cyto}$ induced by the step change of extracellular Ca^{2+} concentration from 1 to 6 mM ($[Ca^{2+}]_{out}$). The state of filling of agonist-sensitive sequestered Ca^{2+} pools was evaluated by the addition of 10 μM carbachol. The state of membrane permeability after the addition of carbachol was evaluated in panels B and D by a step change of extracellular Ca^{2+} concentration from 1 to 6 mM. The boxes above the panels indicate the times and lengths of changes in extracellular Ca^{2+} ($[Ca^{2+}]_{out}$) or addition of 10 μM carbachol during Ca^{2+} measurements in the fluorimeter cuvette. A representative experiment from a series of four is shown.

extracellular medium after carbachol stimulation in HT29 cells provoked a new significant increase in the Ca^{2+} concentration in infected, as well as in mock-infected, cells (Fig. 1B). The amplitude was 36.7 ± 16.0 nM for mock-infected cells, 144 ± 23 nM for SA11 WT-infected cells, and 480 ± 135 nM for SA11 clone 28-infected cells. In all three cases, these changes were significantly larger than those observed before carbachol stimulation (mock infected, 6.1 ± 1.1 nM; SA11 WT, 80 ± 27 nM; SA11 clone 28, 304 ± 65 nM). Similar results were observed in Cos-7 cells after the ATP response. The amplitude values for Cos-7 cells before and after ATP addition were 17.1 ± 3.7 nM versus 56.7 ± 11.0 nM for mock-infected cells, 48.8 ± 5.5 nM versus 110.3 ± 43.4 nM for SA11 WT, and 61.0 ± 16.0 nM versus 119.4 ± 57.1 nM for SA11 clone 28. In the case of mock-infected cells, the small increase was statistically significant and reflects an increase of Ca^{2+} permeability due to the activation of the capacitative pathway (10). This increase in Ca^{2+} entry was much higher in cells infected by either of the two clones, indicating that in infected cells, two components were activated: the capacitative pathway, due to the agonist action, and a virus-induced pathway.

To assess the roles of glycosylation of proteins other than VP7 in Ca^{2+} homeostasis, we also studied the effects of tunicamycin added at 1 h postinfection. As previously shown (37), treatment with tunicamycin did not modify basal $[Ca^{2+}]_{cyto}$, Ca^{2+} permeability, or the Ca^{2+} response to an agonist in mock-infected HT29 or Cos-7 cells (Fig. 1 and 2). Tunicamycin did not affect the capacitative permeability component observed after carbachol stimulation. The amplitude of the increase upon addition of 5 mM Ca^{2+} to the extracellular medium was not significantly different from that of controls without tunicamycin (54.9 + 31.1 nM versus 36.7 ± 16.0 nM for mock-infected cells with or without an agent) (Fig. 1). Similar results were obtained with Cos-7 cells (not shown).

On the other hand, the inhibitor affected the changes in cell Ca^{2+} homeostasis induced by infection with the two different clones (Fig. 1C and D and 2). It decreased the amplitude and rate of rise of $[Ca^{2+}]_{cyto}$ upon addition of 5 mM Ca^{2+} to the extracellular medium. However, tunicamycin did not reverse the effect of infection on the release of Ca^{2+} by the agonist; rather, it tended to enhance the reduction of the amplitude of the Ca^{2+} spike caused by infection by the two clones in the two cell types (Fig. 1 and 2). This effect was statistically significant for SA11 clone 28. It also reduced Ca^{2+} entry after agonists in HT29 cells infected by both clones with respect to untreated cells (Fig. 1B and D). Similar results were observed in infected Cos-7 cells after the ATP response (not shown).

In previous reports, we showed that Ca^{2+} pools measured as $^{45}Ca^{2+}$ uptake progressively increased during the viral cycle (28). This increase was sensitive to thapsigargin, an inhibitor of the sarco/endoplasmic reticulum Ca^{2+}-ATPase pump, indicating that Ca^{2+} was accumulated in the ER during infection (26). This was also inhibited by tunicamycin treatment, suggesting the participation of either VP7 or NSP4 (37). Figure 3 shows that infection of Cos-7 cells with SA11 WT or clone 28 increased $^{45}Ca^{2+}$ uptake, which was reduced to basal levels by treatment with tunicamycin.

On the other hand, we observed that infection by SA11 clone 28 induced effects on Ca^{2+} homeostasis that were larger than those observed with the WT strain. We do not know the origin of this difference. However, the lack of glycosylation may be associated with a change in the kinetics of virus replication. VP7 is involved in the early interactions with the cell, and the lack of glycosylation may modulate the rate of entry, protein synthesis, and/or assembly.

Characterization of NSP4-EGFP expression in transfected Cos-7 cells. To study the effect of NSP4 on Ca^{2+} homeostasis, we transfected Cos-7 cells with a plasmid coding for the NSP4-EGFP fusion protein. This allowed visualization of the expressed protein in transfected cells by live-cell imaging. We first characterized the transitory expression of the protein by Western blotting and confocal microscopy before proceeding to evaluate aspects of Ca^{2+} homeostasis in these cells.

The expression of NSP4 or NSP4-EGFP was analyzed by SDS-PAGE and Western blotting (Fig. 4). We could observe a

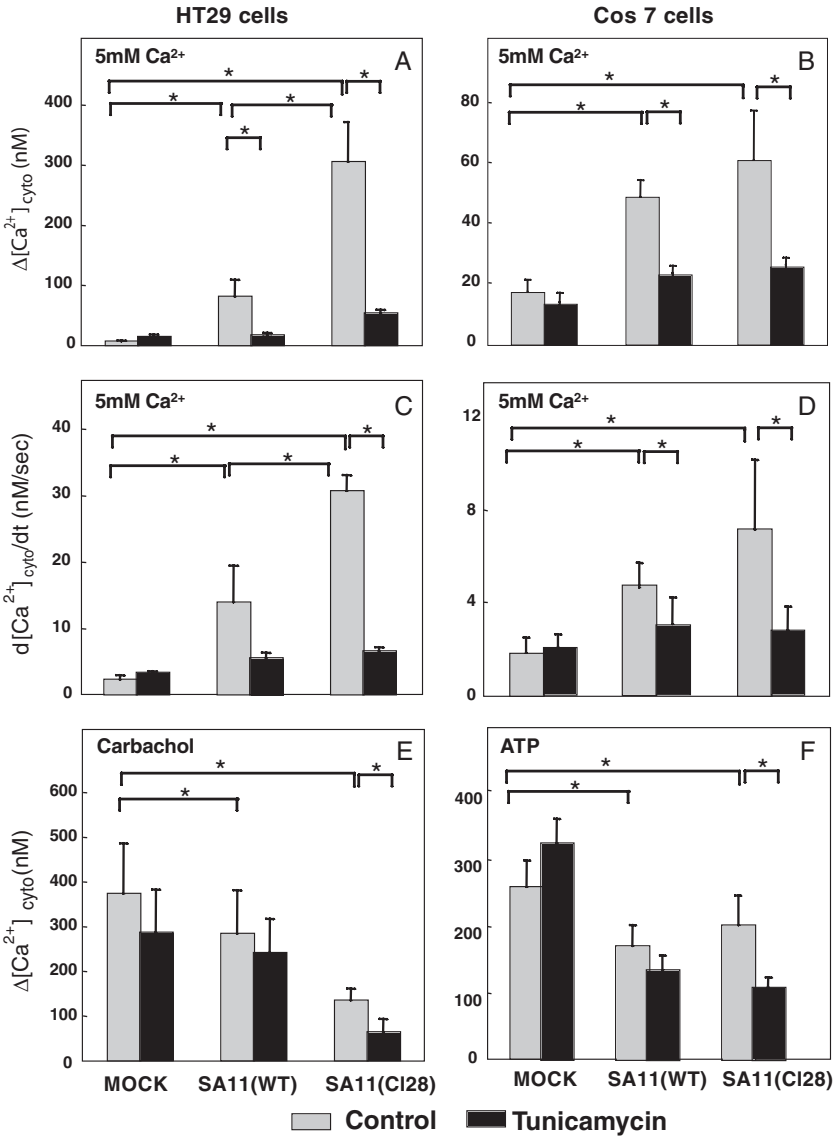

FIG. 2. Analysis of the effects of rotavirus infection with the WT and the variant clone 28 (Cl28) SA11 strains on plasma membrane permeability to Ca^{2+} and agonist-releasable Ca^{2+} pools in HT29 and Cos-7 cells. (A, C, and E) A quantitative study of experiments in HT29 cells performed as for Fig. 1. (B, D, and F) A similar type of experiment in Cos-7 cells. (A and B) The data represent the variation of $[Ca^{2+}]_{cyto}$ induced by the addition of 5 mM Ca^{2+} to the extracellular medium in cells infected or not by the two variants of SA11 in the presence or absence of tunicamycin (protocol as in Fig. 1A and C). (C and D) The bars correspond to the initial rate of $[Ca^{2+}]_{cyto}$ change ($d[Ca^{2+}]/dt$) induced by the addition of 5 mM $CaCl_2$ to the extracellular medium (protocol as in Fig. 1A and C). (E and F) The data correspond to the variation of $[Ca^{2+}]_{cyto}$ induced by the addition of 10 μM carbachol to HT29 cells (protocol as in Fig. 1B and D) or 250 μM ATP to Cos-7 cells. The bars correspond to the means plus SEM of four sets of independent experiments in each series (*, $P < 0.01$; paired t test).

band of around 28 kDa recognized by anti-NSP4 antibodies in the Western blots of lysates of virus-infected cells or cells expressing NSP4 (Fig. 4, lanes 1, 7, and 9). Therefore, expressed NSP4 corresponds to the native rotavirus protein. The expression of the NSP4-EGFP fusion protein was analyzed in cell lysates and after immunoprecipitation with an antibody directed against the C90 peptide of NSP4 (42). We detected a band of around 56 kDa recognized by two different anti-NSP4 antibodies (Fig. 4, lanes 2 to 4), as well as an anti-GFP antibody (Fig. 4, lanes 5 and 6). As the expressed protein had the molecular weight expected for the fusion protein and was recognized by anti-NSP4 and anti-GFP antibodies, it should correspond to NSP4-EGFP.

The digestion of lysates with endo-H induced a migration change of the NSP4 or NSP4-EGFP band to a lower-molecular-weight level, revealing that the NSP4 proteins of rotavirus-infected (Fig. 4, lanes 7 and 8) or -transfected cells (lanes 9 and 10) and the expressed NSP4-EGFP (lanes 11 and 12) were in the glycosylated form.

NSP4-EGFP was detected by fluorescence microscopy as early as 14 h posttransfection. The level of expression gradually increased up to 36 h, when cells started to die. At 24 h post-

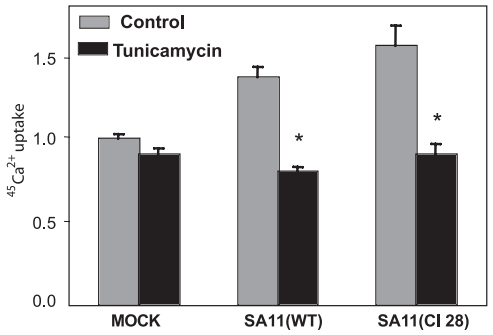

FIG. 3. Effects of infection with the WT and the variant clone 28 (Cl 28) SA11 strains on $^{45}Ca^{2+}$ uptake. Intracellular Ca^{2+} pools were evaluated by $^{45}Ca^{2+}$ uptake in rotavirus (SA11 WT or SA11 Cl 28) or mock-infected cells in the presence or absence of tunicamycin. Confluent monolayers of Cos-7 cells in 24-well plates were mock or rotavirus infected. Tunicamycin (5 μg/ml), when present, was added at 1 h postinfection, and $^{45}Ca^{2+}$ uptake measurements were performed for 10 min at 8 h postinfection. The counts obtained in virus-infected cells were normalized to the values obtained in mock-infected cells. The values correspond to the means (plus SEM) of 20 measurements (five experiments and four replicates for each condition; *, $P < 0.001$; paired t test).

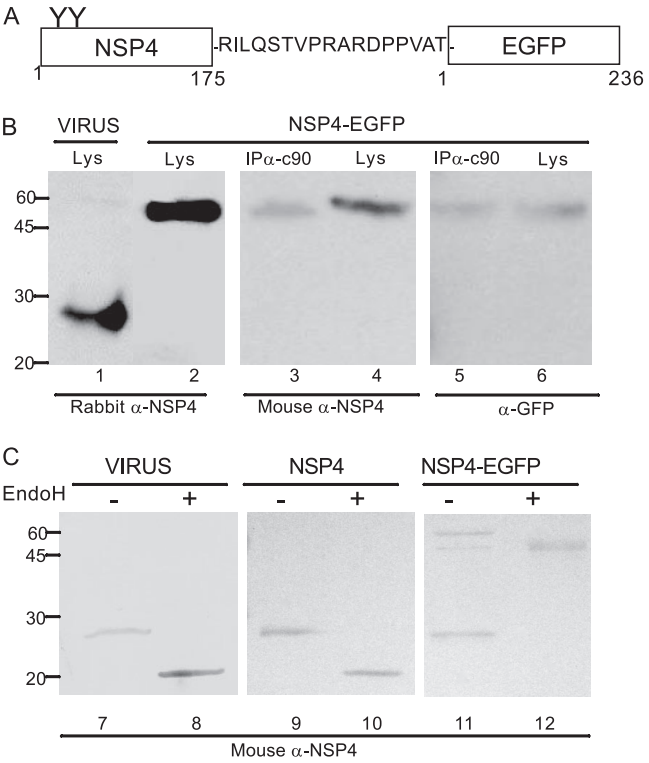

FIG. 4. Analysis of NSP4-EGFP and NSP4 expression by immunoprecipitation and Western blotting. (A) Schematic diagram of NSP4-EGFP fusion protein. (B) Cell lysates of Cos-7 cells infected by RF rotavirus or expressing NSP4-EGFP (24 h posttransfection) were separated by SDS-PAGE and then analyzed by Western blotting using a rabbit antiserum against NSP4 (lanes 1 and 2). Lysates of Cos-7 cells expressing NSP4-EGFP were immunoprecipitated with anti-C90-NSP4 (see Materials and Methods). The lysates (Lys) and immunoprecipitated proteins were analyzed by Western blotting using mouse monoclonal antibody against NSP4 (B4-2; lanes 3 and 4) or an anti-GFP antibody (lanes 5 and 6). (C) Lysates of Cos-7 cells infected by rotavirus (lanes 7 and 8) expressing NSP4 (lanes 9 and 10) or NSP4-EGFP (lanes 11 and 12) were digested (lanes 8, 10, and 12) or not (lanes 7, 9, and 11) with endo-H, separated by SDS-PAGE, and analyzed by Western blotting using mouse monoclonal antibody against NSP4 (B4-2).

transfection, we could observe by confocal microscopy that 60 to 70% of the cells emitted green fluorescence, which was localized in the nuclear envelope and the perinuclear region following a reticular pattern (Fig. 5, rows 1, 2, and 3). We have to point out that after 30 h of transfection a punctate pattern of fluorescence could frequently be seen (Fig. 6, upper right). The expressed protein was recognized by an anti-NSP4 antibody, showing a high degree of colocalization between the green fluorescence of the EGFP moiety and the red immunofluorescence (Fig. 5, row 1). Some points inside the cell had a higher intensity of red immunofluorescence, which might correspond to recognition of degraded NSP4-EGFP by the antibody. The fusion protein was distributed in a reticular compartment also labeled by Bodipy TR-X thapsigargin, which specifically binds to SERCA pumps of the ER (Fig. 5, row 2). This confirms that NSP4-EGFP was being synthesized in the ER. However, the distribution was not uniform, and there were zones of the ER in which NSP4-EGFP was less abundant. When cells were cotransfected with separate plasmids encoding NSP4 and EGFP, NSP4 was observed in the ER, whereas EGFP was directed to the nucleus (Fig. 5, row 5). This indicates that the NSP4 moiety of the protein directs its synthesis and targeting. Expressed NSP4-EGFP and NSP4 in transfected cells had distributions similar to that of NSP4 expressed in cells infected by the RF rotavirus strain (Fig. 5, row 4).

Expression of NSP4-EGFP alters Ca^{2+} homeostasis. The effects of expression of NSP4-EGFP on Ca^{2+} permeability and $[Ca^{2+}]_{cyto}$ were studied in individual cells of a transfected monolayer grown on glass coverslips and loaded with fura-2 (Fig. 6). The selection of cells for $[Ca^{2+}]_{cyto}$ measurement was performed on the basis of NSP4-EGFP fluorescence, choosing those that emitted a diffuse signal with an intermediate intensity and that did not display a punctate pattern (Fig. 6, upper right) to minimize any concentration-dependent interference of EGFP in the fura-2 signal (6). The punctate pattern of distribution of NSP4-EGFP has been previously reported and may correspond to accumulation of the protein in autophagosomes at later times postinfection or -transfection (5). The results are presented as the ratio of fura-2 fluorescence measured at 350- and 380-nm excitation wavelengths, which is a function of $[Ca^{2+}]_{cyto}$. In the left-hand panels, the traces correspond to measurements in individual mock-infected cells, RF virus-infected cells, or NSP4-EGFP-expressing cells. The lower right-hand panel depicts the average trace (± standard error of the mean [SEM]) for each condition in 12 to 15 cells in a single monolayer. (For a statistical analysis of the changes in the fura-2 ratio for a series of experiments performed on different monolayers, see Fig. 8.)

Cells expressing NSP4-EGFP, as well as rotavirus-infected cells, showed a significant increase in the basal fura-2 ratio compared to the mock-infected cells (Fig. 6; see Fig. 8A). Changing the Ca^{2+} concentration in the superfusing medium from 1 to 5 mM induced a prompt increase in the fura-2 ratio, which reached a plateau in both NSP4-EGFP-expressing cells

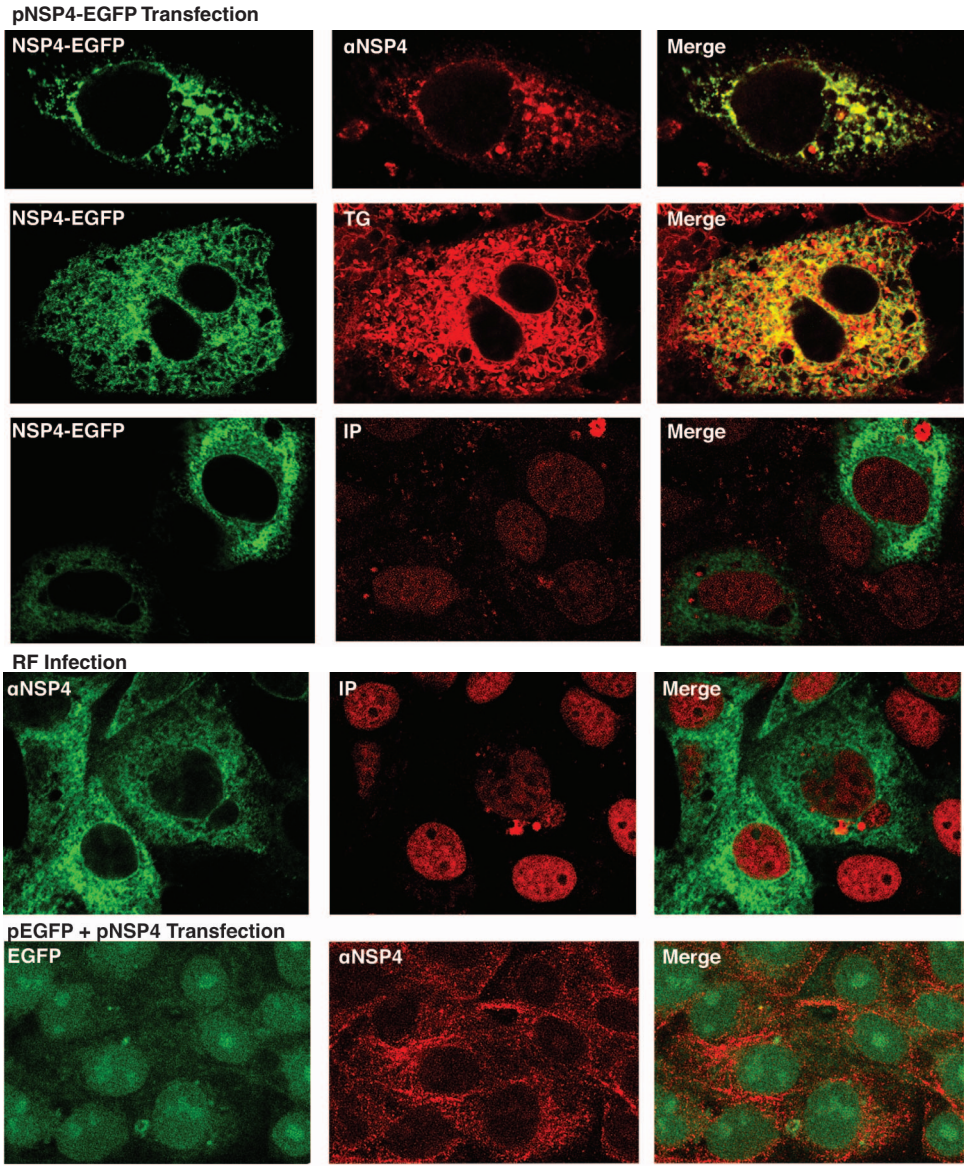

FIG. 5. Characterization of NSP4-EGFP expression in transfected cells by confocal microscopy. Cos-7 cells were grown to 90% confluence on glass coverslips and transfected with different plasmids for the transient expression of NSP4-EGFP, NSP4, or EGFP or infected with rotavirus strain RF. In row 1 (from the top), the green fluorescence of NSP4-EGFP is colocalized with the red fluorescence of anti-NSP4 monoclonal antibody labeled by secondary antibody coupled to Cy3. In row 2, live cells expressing NSP4-EGFP are colocalized in a compartment labeled by Bodipy TR-X thapsigargin (red). Row 3 shows differential localization of NSP4-EGFP and propidium iodide (IP). Row 4 corresponds to cells infected with rotavirus strain RF (7 h postinfection). The cells were immunostained with anti-NSP4 monoclonal antibody labeled by secondary antibody coupled to fluorescein isothiocyanate and treated with propidium iodide (IP). In row 5, cells were cotransfected with separate plasmids encoding NSP4 and EGFP. NSP4 was revealed with anti-NSP4 monoclonal antibody labeled by secondary antibody coupled to Cy3. Green fluorescence corresponding to EGFP was directed to the nucleus.

and rotavirus-infected cells. The increase in the initial rate and amplitude were significant (see Fig. 8A and B). The fluorescence signal returned to basal levels when extracellular [Ca^{2+}] was restored to 1 mM. In the case of mock-infected cells, no significant change in the fura-2 ratio was observed during these manipulations. These results indicate that expression of NSP4-EGFP induces an increase in Ca^{2+} permeability similar to that effected by virus infection.

To evaluate the amount of Ca^{2+} in the ER that was releasable by an agonist, we subsequently added ATP in the presence of 1 mM Ca^{2+}. The agonist provoked a transitory augmentation of the fura-2 ratio in mock-infected cells. In NSP4-EGFP-expressing cells, as well as in virus-infected cells, there was a significant reduction of the Ca^{2+} response to ATP (Fig. 6; see Fig. 8C). These results confirm our previous findings in other cell lines (HT29 and MA104) infected with different rotavirus strains (OSU and SA11) (26, 28, 32, 37) and suggest that the expression of NSP4 is responsible for these effects.

It was essential to our contention to show that the effect was due to the NSP4, but not the EGFP, moiety of the fusion

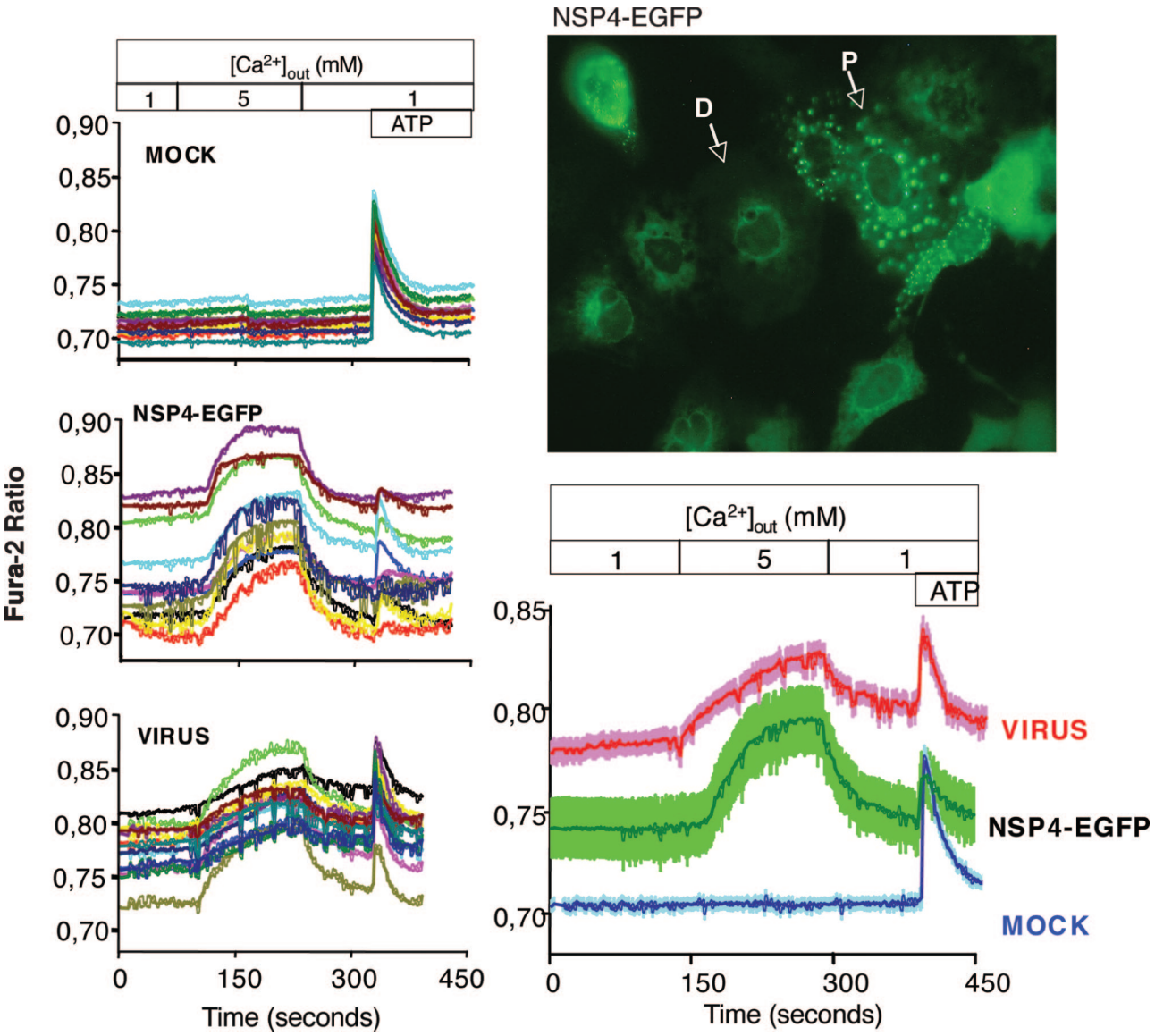

FIG. 6. Changes in the fura-2 ratio as an indication of $[Ca^{2+}]_{cyto}$ induced by NSP4-EGFP expression and rotavirus infection in Cos-7 cells. Cos-7 cells grown on glass coverslips were infected with the RF strain or transfected with the pEGFP-N1NSP4 plasmid as described in Materials and Methods. The mock condition refers to uninfected or untransfected monolayers treated with Lipofectamine 2000. At 7 h postinfection or 24 h posttransfection, the cells were loaded with fura-2–AM, and the coverslips were mounted in a flowthrough perfusion microscope chamber in an inverted fluorescence microscope for fura-2 fluorescence measurements. In the upper right panel, the NSP4-EGFP fluorescence of transfected cells shows a diffuse (D) or punctate (P) pattern. Fura-2 fluorescence measurements were performed in cells presenting a diffuse NSP4-EGFP fluorescence for transfected cells or randomized for rotavirus- or mock-infected cells. The results are presented as the ratio of fura-2 fluorescence measured at 350- and 380-nm excitation wavelengths (see Materials and Methods). Permeability to Ca^{2+} was evaluated by monitoring the change in the fura-2 ratio upon switching solutions from 1 mM to 5 mM $CaCl_2$. The state of filling of agonist-sensitive sequestered Ca^{2+} pools was evaluated by the addition of ATP (250 μM). In the left-hand panels, the traces correspond to measurements in individual mock-infected, rotavirus-infected, or NSP4-EGFP-expressing cells. The lower right-hand panel depicts the average trace (± SEM; light colors) for each condition (mock, $n = 12$; virus, $n = 14$; NSP4-EGFP, $n = 11$). A representative experiment from a series of four is shown.

protein. Therefore, we transfected cell monolayers with plasmids carrying either the NSP4 or the EGFP gene (Fig. 7A and B). In the case of cells transfected with the NSP4 plasmid, selection of cells for Ca^{2+} measurements was done randomly, since no fluorescent reporter was present. The change in extracellular Ca^{2+} from 1 to 5 mM provoked a significant increase in the fura-2 ratio, revealing an increase in the Ca^{2+} permeability of cells transfected with the NSP4 plasmid similar to that observed in cells expressing NSP4-EGFP (Fig. 7A and 8A and B). Equally, these cells showed a significantly reduced Ca^{2+} response to ATP, suggesting that all of the selected cells had been transfected (Fig. 7A and 8C). On the other hand, the expression of EGFP alone or of EGFP-VP4, another fusion protein carrying rotavirus VP4 fused to EGFP, did not modify the Ca^{2+} permeability or the Ca^{2+} response to ATP (Fig. 7B and 8). Therefore, the effects of NSP4-EGFP expression on

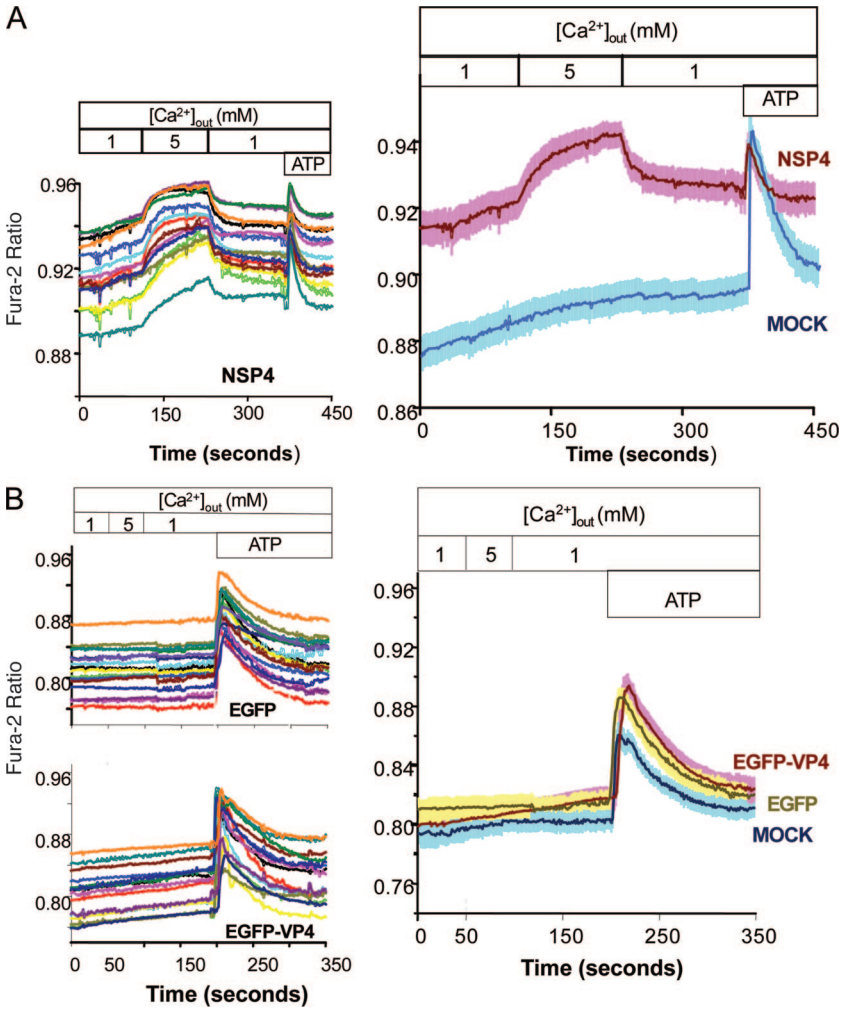

FIG. 7. Effects, of NSP4, EGFP-VP4, and EGFP expression and rotavirus infection on the fura-2 ratio in Cos-7 cells. Cos-7 cells were transiently transfected with plasmids encoding NSP4 (A) or EGFP or EGFP-VP4 (B) for 24 h. The cells were then processed for Ca^{2+} measurements as for Fig. 6. The traces on the left correspond to fura-2 ratio measurements in 13 individual NSP4-expressing cells (A) and 15 individual EGFP- or EGFP-VP4-expressing cells (B). On the right are depicted the average traces (± SEM; light colors) for NSP4- or EGFP- and EGFP-VP4-expressing cells. An average trace (± SEM; light colors) is presented for mock conditions. A representative experiment is shown.

Ca^{2+} homeostasis in transfected cells can be ascribed to the NSP4 moiety.

To see whether there was a relationship between the increase in Ca^{2+} permeability and the NSP4-EGFP expression level, we evaluated the initial rate [d(ratio)/dt] and amplitude of the change in the fura-2 ratio upon increase of the extracellular [Ca^{2+}] in individual cells presenting different EGFP fluorescence intensities (Fig. 9). We could observe that the rate and amplitude of change in the fura-2 ratio with the addition of 5 mM Ca^{2+} to the medium was a linear function of the intensity of green fluorescence, with a high correlation coefficient (R = 0.95) (Fig. 9A and B). This reveals a tight relationship between the level of expression of NSP4-EGFP and the increase in the plasma membrane Ca^{2+} permeability of transfected cells. Regarding the response to ATP in NSP4-EGFP-expressing cells, we could not show a linear relationship between the level of expression (EGFP fluorescence) and the reduction of the Ca^{2+} spike (results not shown).

We then measured $^{45}Ca^{2+}$ uptake to evaluate the total Ca^{2+} contained in the cell (Fig. 10). The expression of NSP4 or NSP4-EGFP (30 h posttransfection) induced a significant increase in $^{45}Ca^{2+}$ uptake, to the same level attained with rotavirus infection (8 h postinfection), whereas EFGP expression showed no effect (Fig. 10A). Thapsigargin added 30 min before the end of the transfection or infection period inhibited this increase, indicating a release of Ca^{2+} from the ER, which had been accumulated during infection or transfection. The increases in $^{45}Ca^{2+}$ uptake were prevented by treatment with tunicamycin added at 1 h postinfection or 10 h posttransfection (Fig. 10B). These results indicate that NSP4 is involved in the increase of Ca^{2+} sequestered in the ER during virus infection.

DISCUSSION

In previous work, we showed that rotavirus infection of cultured cells affects several of the mechanisms that intervene in the control of cytosolic Ca^{2+} concentration. The primary events are an uncompensated increase in Ca^{2+} permeability of

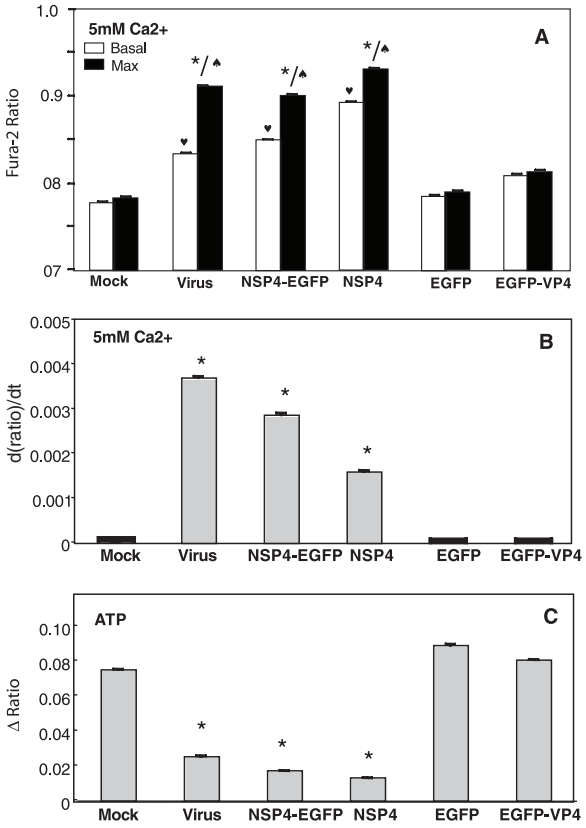

FIG. 8. Analysis of the effects of NSP4-EGFP, NSP4, EGFP-VP4, or EGFP expression and rotavirus infection on the fura-2 ratio in Cos-7 cells and on plasma membrane permeability to Ca^{2+} and agonist-releasable Ca^{2+} pools in Cos-7 cells. (A, B, and C) Analysis of experiments performed as for Fig. 6 and 7. (A) Data representing the fura-2 ratio before (Basal) and after (Max) the addition of 5 mM Ca^{2+} to the extracellular medium. (B) The bars correspond to the initial rates of fura-2 ratio change [d(ratio)/dt] induced by the addition of 5 mM $CaCl_2$ to the extracellular medium (protocol as in Fig. 6A and 7A). (C) The data correspond to the amplitude of the Ca^{2+} spike (Δ ratio) induced by the addition of 250 μM ATP to Cos-7 cells. The bars correspond to the means plus SEM of *n* values; *n* (cells/days) = 60/4 (Mock), 45/3 (Virus), 55/4 (NSP4-EGFP), 30/2 (NSP4), 32/2 (EGFP), 30/2 (EGFP-VP4). Statistical analysis was performed using Student's *t* test. In panel A, the symbols are as follows: ∗, significant difference ($P < 0.001$, at least) between the basal ratio under experimental conditions (virus or transfected) and controls (mock); ♥, significant difference ($P < 0.001$, at least) between the maximal ratio under experimental conditions (virus or transfected) and controls (mock); ♠, significant difference ($P < 0.001$, at least) between the basal and maximal ratios (before and after 5 mM Ca^{2+}) under each experimental condition. In panels B and C, ∗ indicates a significant difference ($P < 0.001$, at least) between values under experimental conditions (virus or transfected) and controls (mock). Nonsignificant differences have no symbols.

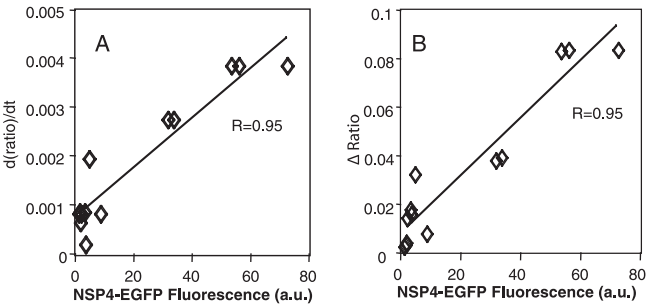

FIG. 9. Relationship between changes in the fura-2 ratio and the level of expression of NSP4-EGFP. Cos-7 cells grown on glass coverslips were transfected with the pEGFP-N1NSP4 plasmid. At 24 h posttransfection, the cells were loaded with fura-2. First, an image of the field was captured at excitation/emission wavelengths of 500/535 nm to measure the intensity of green fluorescence of NSP4-EGFP for each cell selected for fura-2 ratio measurement. Quantification of the fluorescence emitted by the EGFP group in individual cells was performed on images using ImageJ software. To evaluate the Ca^{2+} permeability of the plasma membrane, we followed the same protocol as for Fig. 6. (A) Plot of the initial rate of ratio increase [d(ratio)/dt] as a function of the intensity of green fluorescence. (B) Plot of the amplitude of the peak ratio induced by the increase in the extracellular Ca^{2+} concentration ($[Ca^{2+}]_{out}$) from 1 to 5 mM Ca^{2+} as a function of the intensity of green fluorescence. Each point corresponds to the measurement of an individual cell of the same monolayer ($n = 13$). A representative experiment from a series of two is shown. *R*, correlation coefficient. a.u., arbitrary units.

the plasma membrane and Ca^{2+} entry (28, 32, 36), which lead to an elevation of $[Ca^{2+}]_{cyto}$ and of sequestered Ca^{2+} sensitive to thapsigargin (26). The result is a progressive rise in the $[Ca^{2+}]_{cyto}$. These effects have been demonstrated in different cell lines (monkey kidney MA104 and MDCK and human colon HT29 and Caco2) infected by the porcine OSU or rhesus RRV strain (8, 28, 32, 36). In this work, we extended our observations to monkey kidney Cos-7 cells and two other strains (bovine RF and simian SA11) and observed changes that were qualitatively the same. Nevertheless, it is difficult to make a quantitative comparison of the kinetics and amplitude of changes between the different studies, since numerous parameters influence the infection.

The increase in the Ca^{2+} permeability of the plasma membrane seems to be associated with the synthesis of a viral glycoprotein and not a cellular de novo product (28, 37). This left the question open as to the involvement of VP7 and/or NSP4 in these effects. We took advantage of a variant of the rotavirus SA11 strain, SA11 clone 28, which has an unglycosylated VP7 (16). The fact that infection by SA11 clone 28 induced the same effects on Ca^{2+} homeostasis as the strain with a glycosylated VP7 indicates that glycosylation of this protein is not required to induce the changes linked to rotavirus infection. Furthermore, the inhibition by tunicamycin of the increase in Ca^{2+} permeability and $^{45}Ca^{2+}$ pools in cells infected by SA11 clone 28 reveals that VP7 is not the target of this drug. This suggests that VP7 may not be responsible for the effects of infection on Ca^{2+} permeability. However, taking another approach, it was recently shown that the silencing of VP7 expression partially inhibited the increase in Ca^{2+} permeability in infected cells whereas the silencing of NSP4 completely blocked this effect (46). However, the silencing of VP7 also reduced the synthesis of NSP4 in Cos-7 cells and impaired the assembly of viral particles within the ER (46). This may suggest that reduction of Ca^{2+} permeability in VP7-silenced cells is caused by the reduction of NSP4 synthesis. Furthermore, the accumulation of immature particles in the ER may be linked to a blockade of the trafficking of NSP4 to the membrane and activation of Ca^{2+} permeability. Therefore, the effects of the silencing of VP7 may be indirect by interfering with the synthesis and targeting of NSP4. On the other hand,

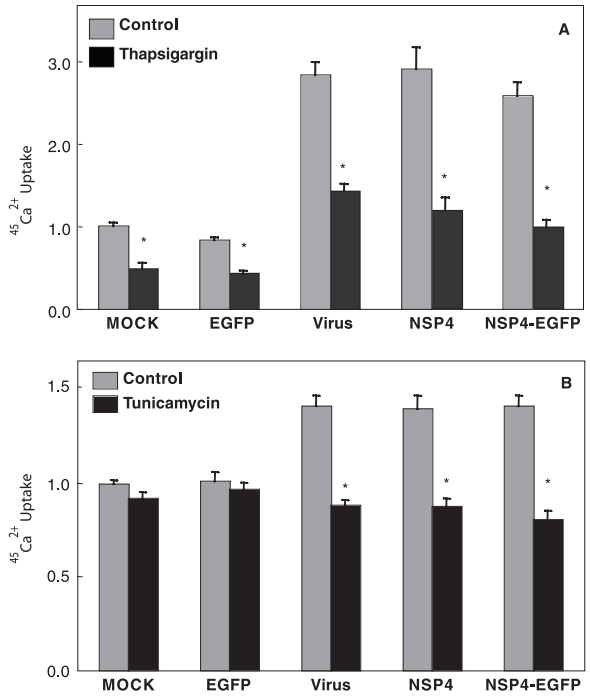

FIG. 10. Effects of NSP4 expression on $^{45}Ca^{2+}$ uptake in transfected cells. Cos-7 cells grown in 24-well plates were transiently transfected with plasmids encoding NSP4-EGFP, NSP4, or EGFP for 30 h or were infected with RF rotavirus for 8 h. Thapsigargin (3 μM) was added 30 min before measurement at the end of the transfection or infection period (A). Tunicamycin (5 μg/ml) was added at 10 h post-transfection or 1 h postinfection (B). The time of $^{45}Ca^{2+}$ uptake was 10 min. The counts obtained in virus-infected or -transfected cells were normalized to those for uninfected and untransfected cells. The values correspond to the means plus SEM of 6 measurements (two independent experiments with three replicates) (A) and 12 measurements (four independent experiments with three replicates) (B). *, $P < 0.001$ (paired t test).

the fact that the silencing of NSP4 completely ablated the increase of Ca^{2+} permeability indicates that NSP4 is sufficient to elicit the effect.

We studied the participation of NSP4 in the changes in Ca^{2+} homeostasis, using a transient expression system for NSP4-EGFP and NSP4 in Cos-7 cells. The expressed NSP4-EGFP or NSP4 presented properties of antigenicity and localization characteristic of the NSP4 protein of infected cells. The expressed NSP4-EGFP and NSP4 proteins had the expected molecular masses (~56 kDa and 28 kDa, respectively), were recognized by three different antibodies against NSP4 in Western blots and immunofluorescence assays, and were both glycosylated. The intracellular distribution of NSP4-EGFP in transfected Cos-7 cells was similar to that of NSP4 synthesized during rotavirus infection. The localization was predominantly reticular in the nuclear envelope and perinuclear region, compatible with ER cisternae. This was confirmed by colocalization in live cells of NSP4-EGFP and fluorescent thapsigargin, a marker of the ER compartment (34). This indicates that the intracellular distribution was guided by the NSP4 moiety and not EGFP, which is directed to the nucleus.

The similarities between the expressed proteins and NSP4 of infected cells permitted the use of the transfection system to undertake physiological studies regarding Ca^{2+} metabolism in these cells. We found that the expression of NSP4-EGFP provoked an increase in plasma membrane Ca^{2+} permeability and $[Ca^{2+}]_{cyto}$ as measured by fura-2 fluorescence. We found a tight correlation between the changes in Ca^{2+} permeability and the level of protein expression at the single-cell level. Furthermore, the increase in Ca^{2+} permeability was specifically due to the action of the NSP4 moiety of the fusion protein, since it was also elicited by transfection of the NSP4 gene alone and was not brought about by expression of either EGFP or EGFP-VP4. Moreover, these effects on Ca^{2+} metabolism were almost identical to those produced by rotavirus infection.

Our results are in accordance with the observation of increased $[Ca^{2+}]_{cyto}$ caused by the inducible expression of NSP4-EGFP in HEK 293 cells (6). However, in the present paper, we also show that this effect, induced by NSP4-EGFP or NSP4 alone, is due to the increase in Ca^{2+} permeability, which in turn triggers an increase in the ER Ca^{2+} content in the same manner as produced by virus infection.

In cells loaded with fura-2, NSP4-EGFP or NSP4 expression led to a decrease in the amplitude of the Ca^{2+} spike elicited by ATP, which liberates Ca^{2+} from the ER. At the same time, the total Ca^{2+} content of the ER (also sensitive to thapsigargin) measured by $^{45}Ca^{2+}$ uptake was enhanced. These effects were identical to those observed during rotavirus infection. To explain these apparently contradictory results, we have previously proposed that there is an increase in the buffer capacity in the ER during infection by viral and cellular proteins, which would decrease the pool that can be mobilized by the agonist (37, 45). The reduction of $^{45}Ca^{2+}$ uptake by the silencing of VP7 or NSP4 supports this contention (46). However, this hypothesis remains to be investigated.

On the other hand, the reduction of agonist-mobilizable Ca^{2+} pools in infected cells or NSP4-EGFP-expressing cells might be the consequence of an increase in ER membrane Ca^{2+} permeability, as has been proposed (43). This in turn would lead to the activation of the capacitative pathway and Ca^{2+} entry. However, this is in conflict with the increase in $^{45}Ca^{2+}$ uptake. Furthermore, the capacitative pathway represents a small fraction of the total increase in Ca^{2+} permeability and is not inhibited by tunicamycin, as shown for the viral component (37).

Our results support the hypothesis that NSP4 expressed during infection is responsible for the changes in Ca^{2+} homeostasis. Different explanations may account for these effects. NSP4 may increase Ca^{2+} permeability directly by forming a plasma membrane Ca^{2+} channel. The viral protein would traffic from the ER to the plasma membrane, where this channel would become active through unknown mechanisms, such as conformational changes, oligomerization, and/or proteolysis. In spite of the fact that NSP4 is synthesized in the ER membrane, the activation of the putative channel would take place out of this compartment, since during infection there is an increase in total Ca^{2+} in the ER.

Supporting this view, a truncated form of recombinant NSP4 expressed in Vero cells corresponding to the transmembrane segment of the molecule (1 to 89 aa) was able to escape the ER via a brefeldin A-sensitive pathway and reach the plasma membrane (29). On the other hand, the full-length, glycosylated NSP4 molecule has recently been de-

tected in plasma membrane rafts interacting with caveolin in rotavirus-infected or NSP4-EGFP-expressing cells (41). In this case, the trafficking of NSP4 involved a Golgi apparatus-bypassing transport as judged from its endo-H sensitivity. However, the inhibitory effect of brefeldin A on the increase of permeability elicited by infection, which we reported previously, supports the involvement of a Golgi apparatus-dependent pathway (37). It is interesting that the full-length NSP4 molecule was secreted via a brefeldin A-sensitive pathway in Caco2 cells (9). Whether NSP4 secretion, localization at the plasma membrane, and the increase in Ca^{2+} permeability are related phenomena remains to be investigated.

Alternatively, NSP4 could induce Ca^{2+} entry by activating a cellular Ca^{2+} pathway at the plasma membrane. We may discard at this point the activation of the capacitative pathway induced by store depletion, since it cannot explain the magnitude of the change in Ca^{2+} permeability elicited by rotavirus infection (37).

Within our hypothesis, NSP4 would be acting as a viroporin (19). These viral proteins have a hydrophobic transmembrane domain that interacts with the lipid bilayer, forming hydrophilic pores by oligomerization, giving rise to enhanced passage of ions and small molecules (17, 19). NSP4 has a hydrophobic domain that spans the membrane, and it has been shown to undergo oligomerization under certain conditions (4, 7, 42). The topology of NSP4 at a putative site in the plasma membrane remains to be elucidated. The mechanisms of Ca^{2+} passage induced by this protein in rotavirus-infected cells are currently under investigation.

ACKNOWLEDGMENTS

We are grateful to M. K. Estes for providing the SA11 clone 28 rotavirus strain. Philippe Fontanges provided expert technical assistance.

This project was supported by the Consejo Nacional de Investigaciones Científicas y Tecnologicas (FONACIT), Venezuela, through grants S1-2001000329, G2001000637, and F2005000222; by the FONACIT-ECOSNORD international program (PI 2002000905); and by TOTAL Venezuela S.A. and Laboratorios Chacao.

REFERENCES

1. **Altenburg, B. C., D. Y. Graham, and M. K. Estes.** 1980. Ultrastructural study of rotavirus replication in cultured cells. J. Gen. Virol. **46:**75–85.
2. **Au, K. S., W. K. Chan, J. W. Burns, and M. K. Estes.** 1989. Receptor activity of rotavirus nonstructural glycoprotein NS28. J.Virol. **63:**4553–4562.
3. **Ball, J. M., P. Tian, C. Q. Zeng, A. P. Morris, and M. K. Estes.** 1996. Age-dependent diarrhea induced by a rotaviral nonstructural glycoprotein. Science **272:**101–104.
4. **Bergmann, C. C., D. Maass, M. S. Poruchynsky, P. H. Atkinson, and A. R. Bellamy.** 1989. Topology of the non-structural rotavirus receptor glycoprotein NS28 in the rough endoplasmic reticulum. EMBO J. **8:**1695–1703.
5. **Berkova, Z., S. E. Crawford, G. Trugnan, T. Yoshimori, A. P. Morris, and M. K. Estes.** 2006. Rotavirus NSP4 induces a novel vesicular compartment regulated by calcium and associated with viroplasms. J. Virol. **80:**6061–6071.
6. **Berkova, Z., A. P. Morris, and M. K. Estes.** 2003. Cytoplasmic calcium measurement in rotavirus enterotoxin-enhanced green fluorescent protein (NSP4-EGFP) expressing cells loaded with Fura-2. Cell Calcium **34:**55–68.
7. **Bowman, G. D., I. M. Nodelman, O. Levy, S. L. Lin, P. Tian, T. J. Zamb, S. A. Udem, B. Venkataraghavan, and C. E. Schutt.** 2000. Crystal structure of the oligomerization domain of NSP4 from rotavirus reveals a core metal-binding site. J. Mol. Biol. **304:**861–871.
8. **Brunet, J. P., J. Cotte-Laffitte, C. Linxe, A. M. Quero, M. Geniteau-Legendre, and A. Servin.** 2000. Rotavirus infection induces an increase in intracellular calcium concentration in human intestinal epithelial cells: role in microvillar actin alteration. J Virol **74:**2323–2332.
9. **Bugarcic, A., and J. A. Taylor.** 2006. Rotavirus nonstructural glycoprotein NSP4 is secreted from the apical surfaces of polarized epithelial cells. J. Virol. **80:**12343–12349.
10. **Carafoli, E.** 2002. Calcium signaling: a tale for all seasons. Proc. Natl. Acad. Sci. USA **99:**1115–1122.
11. **Chemello, M. E., O. C. Aristimuno, F. Michelangeli, and M. C. Ruiz.** 2002. Requirement for vacuolar H^+-ATPase activity and Ca^{2+} gradient during entry of rotavirus into MA104 cells. J. Virol. **76:**13083–13087.
12. **Ciarlet, M., J. E. Ludert, and F. Liprandi.** 1995. Comparative amino acid sequence analysis of the major outer capsid protein (VP7) of porcine rotaviruses with G3 and G5 serotype specificities isolated in Venezuela and Argentina. Arch. Virol. **140:**437–451.
13. **Cohen, J., J. Laporte, A. Charpilienne, and R. Scherrer.** 1979. Activation of rotavirus RNA polymerase by calcium chelation. Arch. Virol. **60:**177–186.
14. **Dong, Y., C. Q. Zeng, J. M. Ball, M. K. Estes, and A. P. Morris.** 1997. The rotavirus enterotoxin NSP4 mobilizes intracellular calcium in human intestinal cells by stimulating phospholipase C-mediated inositol 1,4,5-trisphosphate production. Proc. Natl. Acad. Sci. USA **94:**3960–3965.
15. **Estes, M. K.** 1996. Rotaviruses and their replication, p. 1625–1655. *In* B. N. Fields, P. M. Knipe, P. M. Howley, R. M. Chanock, J. L. Melnick, T. P. Monath, B. Roizman, and S. E. Straus (ed.), Fields virology, 3ird ed, vol. 2. Lippincott-Raven Publishers, Philadelphia, PA.
16. **Estes, M. K., D. Y. Graham, R. F. Ramig, and B. L. Ericson.** 1982. Heterogeneity in the structural glycoprotein (VP7) of simian rotavirus SA11. Virology **122:**8–14.
17. **Fischer, W. B., and M. S. Sansom.** 2002. Viral ion channels: structure and function. Biochim. Biophys. Acta **1561:**27–45.
18. **Gardet, A., M. Breton, P. Fontanges, G. Trugnan, and S. Chwetzoff.** 2006. Rotavirus spike protein VP4 binds to and remodels actin bundles of the epithelial brush border into actin bodies. J. Virol. **80:**3947–3956.
19. **Gonzalez, M. E., and L. Carrasco.** 2003. Viroporins. FEBS Lett. **552:**28–34.
20. **Grynkiewicz, G., M. Poenie, and R. Y. Tsien.** 1985. A new generation of Ca^{2+} indicators with greater improved fluorescence properties. J. Biol. Chem. **260:**3440–3450.
21. **Jourdan, N., M. Maurice, D. Delautier, A. M. Quero, A. L. Servin, and G. Trugnan.** 1997. Rotavirus is released from the apical surface of cultured human intestinal cells through nonconventional vesicular transport that bypasses the Golgi apparatus. J. Virol. **71:**8268–8278.
22. **Kapikian, A. Z., Y. Hoshino, and R. M. Chanock.** 2001. Rotaviruses, p. 1787–1833. *In* D. M. Knipe and P. M. Howley (ed.), Fields virology, 4th ed, vol. 2. Lippincott Williams & Wilkins Co., Philadelphia, PA.
23. **Ludert, J. E., F. Michelangeli, F. Gil, F. Liprandi, and J. Esparza.** 1987. Penetration and uncoating of rotaviruses in cultured cells. Intervirology **27:**95–101.
24. **Lundgren, O., A. T. Peregrin, K. Persson, S. Kordasti, I. Uhnoo, and L. Svensson.** 2000. Role of the enteric nervous system in the fluid and electrolyte secretion of rotavirus diarrhea. Science **287:**491–495.
25. **Meyer, J. C., C. C. Bergmann, and A. R. Bellamy.** 1989. Interaction of rotavirus cores with the nonstructural glycoprotein NS28. Virology **171:**98–107.
26. **Michelangeli, F., F. Liprandi, M. E. Chemello, M. Ciarlet, and M. C. Ruiz.** 1995. Selective depletion of stored calcium by thapsigargin blocks rotavirus maturation but not the cytopathic effect. J. Virol. **69:**3838–3847.
27. **Michelangeli, F., and M. C. Ruiz.** 2003. Physiology and pathophysiology of the gut in relation to viral diarrhea, p. 23–50. *In* U. Dusselberger and J. Gray (ed.), Viral gastroenteritis, vol. 9. Elsevier, Amsterdam, The Netherlands.
28. **Michelangeli, F., M. C. Ruiz, J. R. del Castillo, J. E. Ludert, and F. Liprandi.** 1991. Effect of rotavirus infection on intracellular calcium homeostasis in cultured cells. Virology **181:**520–527.
29. **Mirazimi, A., K. E. Magnusson, and L. Svensson.** 2003. A cytoplasmic region of the NSP4 enterotoxin of rotavirus is involved in retention in the endoplasmic reticulum. J. Gen. Virol. **84:**875–883.
30. **Morris, A. P., and M. K. Estes.** 2001. Microbes and microbial toxins: paradigms for microbial-mucosal interactions. VIII. Pathological consequences of rotavirus infection and its enterotoxin. Am. J. Physiol. Gastrointest. Liver Physiol. **281:**G303–G310.
31. **Morris, A. P., J. K. Scott, J. M. Ball, C. Q. Zeng, W. K. O'Neal, and M. K. Estes.** 1999. NSP4 elicits age-dependent diarrhea and Ca^{2+} mediated I^- influx into intestinal crypts of CF mice. Am. J. Physiol. **277:**G431–G444.
32. **Perez, J. F., M. C. Ruiz, M. E. Chemello, and F. Michelangeli.** 1999. Characterization of a membrane calcium pathway induced by rotavirus infection in cultured cells. J. Virol. **73:**2481–2490.
33. **Poruchynsky, M. S., D. R. Maass, and P. H. Atkinson.** 1991. Calcium depletion blocks the maturation of rotavirus by altering the oligomerization of virus-encoded proteins in the ER. J. Cell Biol. **114:**651–656.
34. **Ruiz, M. C., O. C. Aristimuno, Y. Diaz, F. Pena, M. E. Chemello, H. Rojas, J. E. Ludert, and F. Michelangeli.** 2007. Intracellular disassembly of infectious rotavirus particles by depletion of Ca^{2+} sequestered in the endoplasmic reticulum at the end of virus cycle. Virus Res. **130:**140–150.
35. **Ruiz, M. C., A. Charpilienne, F. Liprandi, R. Gajardo, F. Michelangeli, and J. Cohen.** 1996. The concentration of Ca^{2+} that solubilizes outer capsid proteins from rotavirus particles is dependent on the strain. J. Virol. **70:**4877–4883.

36. **Ruiz, M. C., J. Cohen, and F. Michelangeli.** 2000. Role of Ca^{2+} in the replication and pathogenesis of rotavirus and other viral infections. Cell Calcium **28:**137–149.
37. **Ruiz, M. C., Y. Diaz, F. Pena, O. C. Aristimuno, M. E. Chemello, and F. Michelangeli.** 2005. Ca^{2+} permeability of the plasma membrane induced by rotavirus infection in cultured cells is inhibited by tunicamycin and brefeldin A. Virology **333:**54–65.
38. **Shahrabadi, M. S., L. A. Babiuk, and P. W. K. Lee.** 1987. Further analysis of the role of calcium in rotavirus morphogenesis. Virology **158:**103–111.
39. **Shahrabadi, M. S., and P. W. K. Lee.** 1986. Bovine rotavirus maturation is a calcium-dependent process. Virology **152:**298–307.
40. **Shirley, J. A., G. M. Beards, M. E. Thouless, and T. H. Flewett.** 1981. The influence of divalent cations on the stability of human rotavirus. Arch. Virol. **67:**1–9.
41. **Storey, S. M., T. F. Gibbons, C. V. Williams, R. D. Parr, F. Schroeder, and J. M. Ball.** 2007. Full-length, glycosylated NSP4 is localized to plasma membrane caveolae by a novel raft isolation technique. J. Virol. **81:**5472–5483.
42. **Taylor, J. A., J. A. O'Brien, and M. Yeager.** 1996. The cytoplasmic tail of NSP4, the endoplasmic reticulum-localized non-structural glycoprotein of rotavirus, contains distinct virus binding and coiled coil domains. EMBO J. **15:**4469–4476.
43. **Tian, P., M. K. Estes, Y. Hu, J. M. Ball, C. Q. Zeng, and W. P. Schilling.** 1995. The rotavirus nonstructural glycoprotein NSP4 mobilizes Ca^{2+} from the endoplasmic reticulum. J. Virol. **69:**5763–5772.
44. **Tian, P., Y. Hu, W. P. Schilling, D. A. Lindsay, J. Eiden, and M. K. Estes.** 1994. The nonstructural glycoprotein of rotavirus affects intracellular calcium levels. J. Virol. **68:**251–257.
45. **Xu, A., A. R. Bellamy, and J. A. Taylor.** 1998. BiP (GRP78) and endoplasmin (GRP94) are induced following rotavirus infection and bind transiently to an endoplasmic reticulum-localized virion component. J. Virol. **72:**9865–9872.
46. **Zambrano, J. L., Y. Diaz, F. Pena, E. Vizzi, M. C. Ruiz, F. Michelangeli, F. Liprandi, and J. E. Ludert.** 2008. Silencing of rotavirus NSP4 or VP7 expression reduces alterations in Ca^{2+} homeostasis induced by infection in cultured cells. J. Virol. **82:**5815–5824.
47. **Zhang, M., C. Q. Zeng, A. P. Morris, and M. K. Estes.** 2000. A functional NSP4 enterotoxin peptide secreted from rotavirus-infected cells. J. Virol. **74:**11663–11670.